International Journal of Applied Earth Observation and Geoinformation 34 (2015) 51–57

Contents lists available at ScienceDirect

International Journal of Applied Earth Observation and Geoinformation

journal homepage: www.elsevier.com/locate/jag

Remote sensing and object-based techniques for mapping fine-scale industrial disturbances

Ryan P. Powers [a,*], Txomin Hermosilla [a], Nicholas C. Coops [a], Gang Chen [b]

[a] Integrated Remote Sensing Studio, Department of Forest Resources Management, University of British Columbia, 2424 Main Mall, Vancouver, BC, Canada V6T 1Z4

[b] Department of Geography and Earth Sciences, University of North Carolina at Charlotte, 9201 University City Boulevard, Charlotte, NC 28223, USA

ARTICLE INFO

Article history:
Received 5 March 2014
Accepted 24 June 2014

Keywords:
Feature extraction
Geographic object-based image analysis (GEOBIA)
Disturbance
Oil sands
Boreal

ABSTRACT

Remote sensing provides an important data source for the detection and monitoring of disturbances; however, using this data to recognize fine-spatial resolution industrial disturbances dispersed across extensive areas presents unique challenges (e.g., accurate delineation and identification) and deserves further investigation. In this study, we present and assess a geographic object-based image analysis (GEOBIA) approach with high-spatial resolution imagery (SPOT 5) to map industrial disturbances using the oil sands region of Alberta's northeastern boreal forest as a case study. Key components of this study were (*i*) the development of additional spectral, texture, and geometrical descriptors for characterizing image-objects (groups of alike pixels) and their contextual properties, and (*ii*) the introduction of decision trees with boosting to perform the object-based land cover classification. Results indicate that the approach achieved an overall accuracy of 88%, and that all descriptor groups provided relevant information for the classification. Despite challenges remaining (e.g., distinguishing between spectrally similar classes, or placing discrete boundaries), the approach was able to effectively delineate and classify fine-spatial resolution industrial disturbances.

Introduction

Successful forest ecosystem management and large area planning requires spatially explicit data on natural resources to inform on forest condition, composition and extent (Desclée et al., 2006). In this regard, the detection and monitoring of disturbances is an integral component to effective forest management, especially in locations like Alberta's boreal forest, where anthropogenic activities greatly contribute to contemporary change (Schneider and Dyer, 2009). While forests do have a natural capacity to re-establish after a disturbance event, the degree of ecological effects (Zager et al., 1983; Archibald et al., 1987; Mace et al., 1996) and rate of regeneration can differ greatly between disturbance types. In the Canadian boreal forest, recovery from periodic natural disturbances such as fire is relatively rapid, with signs of advanced recovery usually taking place within 10 years (Schneider, 2002). In contrast, industrial disturbances associated with the creation of seismic lines can take decades to regenerate (Osko and MacFarlane, 2001), and the establishment of access roads, well sites (i.e., core holes) and pipelines represent a more permanent change. Seismic exploration, for example, is the process of mapping subsurface geology to locate and assess oil and gas reserves by creating seismic lines and recording shock waves. Such industry activities (e.g., forest cutlines, roads, clearings and the operation of large equipment) fragment the landscape and can compact the soil or damage the vegetative mat (Severson-Baker, 2004). The cumulative impacts associated with repeated and/or intensification of seismic surveys (i.e., greater density) by the same or competing companies can also increase environmental damage to affected areas and, subsequently, lead to a longer recovery period (Severson-Baker, 2004).

Given the magnitude and diffuse nature of industrial disturbances across Alberta's boreal forest and the anticipated slow recovery, it is apparent that these human activities have the potential to radically alter the forest ecosystem structure and condition (Schneider and Dyer, 2009); thus, warrant additional monitoring to ensure proper management of the region. Typically, broad, long-term patterns associated with disturbances are identified, detected

* Corresponding author. Tel.: +1 778 997 3646.
E-mail address: rppowers@alumni.ubc.ca (R.P. Powers).

http://dx.doi.org/10.1016/j.jag.2014.06.015
0303-2434/

and mapped using satellite data. To date, the focus of most anthropogenic disturbance studies in boreal areas has been on quantifying the impact of fragmentation (e.g., Hobson and Bayne, 2000; Meddens et al., 2008; Linke et al., 2005) or land cover variation (e.g., Gillanders et al., 2008; Potapov et al., 2011; Schroeder et al., 2011) using Landsat (TM and ETM+) imagery. While these moderate resolution (30 m) analyses are well suited for detecting fragmentation and land cover changes at a patch dimension (~1 ha), they may not be sufficient for detecting finer-scale fragmentation or fine-pattern landscape change. For example, seismic lines, which typically vary between 6 and 8 m in width (GOA, 1998), are much smaller than the 30 m Landsat pixel. On the other hand, high spatial resolution data (<5 m) provides the opportunity to identify fine-spatial resolution elements and patterns (Wulder et al., 2004), but the sensors used to derive the imagery typically compensate the number of spectral bands for increased spatial resolution. With fewer spectral channels, it becomes increasingly challenging to differentiate subtle differences amongst similar land cover types. Given the limitations of both the moderate and fine-spatial resolution imagery, it appears that (*i*) finer spatial resolution imagery (<5 m) are required to isolate physically smaller industrial disturbances, and (*ii*) that additional characterization (e.g., structural and statistical) is needed to more effectively differentiate spectrally similar elements within a scene.

Geographic object based image analysis (GEOBIA) is a useful approach for addressing the two considerations outlined above. Specifically, GEOBIA builds upon the object-based paradigm to include spatial location and context as key components of its analysis (Hay and Castilla, 2008) and allows for more meaningful classification of the landscape than traditional pixel-based image processing methods, especially when high spatial resolution data is used (Blaschke and Strobl, 2001; Benz et al., 2004; Zhou and Troy, 2008). Segmentation, the initial step in GEOBIA, is the partitioning of the scene into a set of jointly exhaustive, discrete regions or objects that are more internally uniform than when compared to their neighbouring objects (Wulder et al., 2008). From these segments it is possible to obtain information about geometry and context, such as size, shape, and topology in addition to spectra, which allows for more accurate and useful classifications (Hay et al., 2005; Johansen et al., 2010; Blaschke et al., 2014). This approach is particularly useful in instances where spectral properties are similar, but the geometry and context are distinct. Seismic lines, for example, are narrow, linear features (i.e., cleared strips of land or cutlines) created in seismic surveys. Like most disturbances, such features can experience many possible successional trajectories based on their particular site conditions (e.g., soil, climate, topography, etc.). Since these trajectories and subsequent land covers are not unique to seismic lines, it is very challenging to consistently identify these features with just spectral information. That said, as long as the geometry of features (e.g., industrial disturbances) are maintained, it provides a distinct set of properties that can be used to identify them irrespective of its land cover appearance (Blaschke et al., 2014). In essence, by classifying the objects (groups of pixels) it is possible to define meaningful image objects based on its unique size, shape and spatial distribution (e.g., individual tree, forest, access road, well site, seismic line, etc.).

The main objective of this study is to assess the application of remote sensing for detecting and subsequently monitoring fine-scale industrial disturbances within the boreal forest of Alberta. To achieve this goal, we (*i*) applied a GEOBIA approach in conjunction with high spatial resolution imagery (2.5 m); (*ii*) incorporated contextual measures in the object-based classification using decision trees and boosting; and (*iii*) compared disturbance effects between ecologically varied study sites.

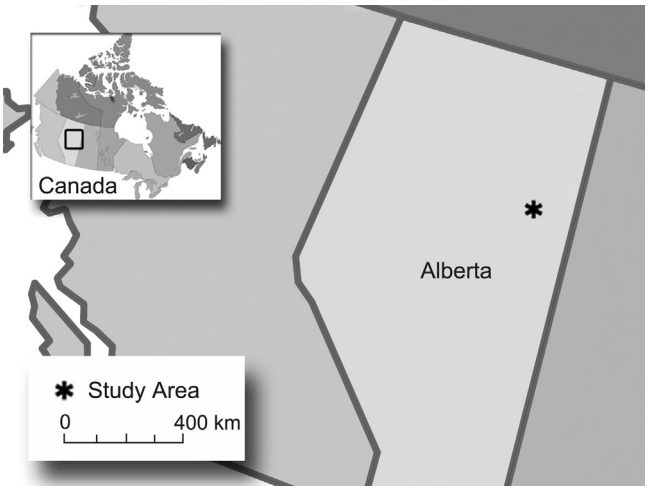

Fig. 1. Study area.

Methods

Study area and data

The study area (Fig. 1) is located in the oil sands region near Fort McMurray, Alberta, Canada, which is approximately 400 km northeast of Edmonton and west of the Saskatchewan border. The extent of the 60 km × 60 km study area is defined by a single SPOT 5 image at N 57°7′56″ to N 56°26′32″ and W 111°30′46″ to W 111°53′49″. Water features such as rivers (i.e., Athabasca River), lakes and wetlands (e.g., bogs, fens, marshes, and aquatic bed) are common. Forested areas include cold tolerant tree species such as Trembling Aspen [*Populus tremuloides* Michx.], Balsam Poplar [*Populus sect. tacamahaca*], White Spruce [*Picea glauca* (Moench) Voss.], White Birch [*Betula pubescens* Ehrh.], Black Spruce [*Picea mariana* (Mill.) Britton, Stems and Poggenburg] and Tamarack [*Larix laricina* (Du Roi) K. Koch], with the latter two species residing mostly in poorly drained wetland areas. This area is dominated by disturbances associated with anthropogenic activities (e.g., oil and gas exploration and extraction). The majority of the oil sands development is concentrated in the northwest; however, other industrial disturbances such as access roads, seismic lines, and well sites are present throughout.

We used a cloud-free SPOT 5 scene acquired on June 29, 2006. The image has an 8-bit radiometric resolution and was obtained at a low angle of incidence (6.8°). It consists of a 2.5 m panchromatic band (0.48–0.71 μm) and four multispectral bands with 10 m spatial resolution for the green (0.50–0.59 μm), red (0.61–0.68 μm), and near infrared bands (0.78–0.89 μm), and a short-wave infrared band (1.58–1.75 μm) with 20 m spatial resolution. The Gram–Schmidt Spectral Sharpening image fusion technique (Laben et al., 2000) combined with cubic convolution interpolation was applied to produce a 2.5 m fused image. Eight ecologically varied sites were selected for classification (Fig. 2).

The object-based classification, described in more detail in the following sections, used 1235 samples (i.e., polygons) for training and testing the classification of five broad classes, which consist of two wetland classes: *bog* (90 reference samples) and *fen* (260) and three upland classes: *forest* (170), *shrub* (218), and *industrial disturbance* (487). These five broad classes, which are functionally different, represent the dominant land covers within the eight ecologically varied study sites. Here the *fen* wetland class comprised of six subclasses (i.e., graminoid poor, shrubby poor, treed poor, graminoid rich, shrubby rich, and treed rich), whereas the *bog*

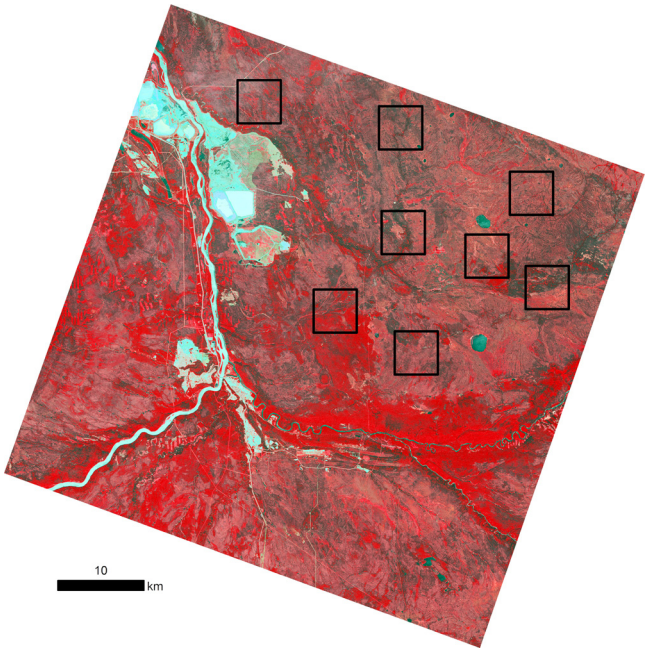

Fig. 2. Spot 5 scene highlighting the eight ecologically varied sites selected for classification.

wetland class was made up of only two subclasses (shrubby and treed). The higher sample rate for the *industrial disturbance* class was attributed to its variety and many subclasses (i.e., seismic lines, well sites, access roads, roads, clearings, and pipelines). Reference data was obtained using a restricted random selection (Chartfield, 1991), which insures the spatial homogeneity of the samples, followed by redistribution and inclusion of additional samples to maintain an appropriate number, with respect to the variability in each category. The average polygon size was 0.14 ± 2.59 ha, with a minimum and maximum size of 0.001 and 444.19 ha, respectively.

Processes

The main steps of the object-based image classification methodology include: segmentation, descriptive attribute extraction, and classification. Image objects were defined by segmenting both the original spectral bands and the normalized difference vegetation index (NDVI) image using a two-step automatic segmentation process based on the *watershed by immersion* algorithm (Vincent and Soille, 1991). Initially, edges were detected using the Sobel edge detection method. This method works by using a directional convolution mask to estimate the gradient in both the horizontal and vertical directions, which combined produce the gradient magnitude image, where the highest pixel values represent areas with the highest pixel contrast (Sobel and Feldman, 1968). A watershed algorithm was then applied over the gradient magnitude image by first sorting the pixels by increasing gradient value, and then "flooding" the image (beginning with the minimum pixel), producing segments with similar pixel intensities. Afterwards, the spectral similarities of the neighbouring segments defined with the watershed algorithm were analyzed, and – in order to avoid over-segmentation issues – those segments with similar properties were merged by applying the full schedule lambda method (Robinson and Redding, 2002). This method works by iteratively merging segments when the merging cost is less than a defined value. The merging cost is computed based on both spectral (i.e., average intensity values for each band) and spatial information (Euclidean distance between adjacent segments). Both steps (segmentation and merging) were driven by two tuning parameters controlling the size and shape of the produced objects, denoted scale level, responsible for the suppression of weak edges, and merge level (i.e. merging cost), computed from the normalized cumulative distribution function.

Descriptive attributes were computed using the object-based image analysis software FETEX 2.0 (Ruiz et al., 2011). In this case, three kinds of topological descriptive attributes were extracted: spectral, textural, and geometrical. Spectral attributes were used to quantify the reflectance response of the objects in the different spectral bands and/or band ratios. Specifically, objects were characterized with the mean, standard deviation, minimum, maximum, range, and mode values of each original band and the NDVI image. Textural attributes measure the spatial distribution of the intensity values within each analyzed object and included: (*i*) contrast, uniformity, entropy, covariance, inverse difference moment, and correlation descriptors (Haralick et al., 1973) derived from the grey-level co-occurrence matrix (GLCM) computed from each object, contrast, uniformity, entropy, covariance, inverse difference moment, and correlation; (*ii*) kurtosis and skewness measures, which are used to characterize the histogram distribution; (*iii*) mean and standard deviation of the *edgeness factor*, which quantified the edge density within a neighbourhood for each pixel composing the object; and (*iv*) experimental semivariogram descriptors close to the origin and from the first maximum proposed by Balaguer-Beser et al. (2013) describing the spatial correlation and patterns: ratio between the values of the total variance and the semivariance at first lag (RVF), ratio between semivariance values at second and first lag (RSF), first derivative near the origin (FDO), second derivative at third lag (SDT), first maximum lag value (FML), mean of the semivariogram values up to the first maximum (MFM), variance of the semivariogram values up to the first maximum (VFM), difference between MFM and the semivariance at first lag (DMF), ratio between the semivariance at first local maximum and the mean semivariogram values up to this maximum (RMM), and second-order difference between first lag and first maximum (SDF). Lastly, the geometrical attributes were used to describe the dimensions and shape of the objects. In this case, attributes were calculated for each object's area, perimeter, elongation, shape index, compactness, fractal dimension, and elongation.

Two analysis levels were defined to extract the descriptive attributes: object and context. The attributes computed at the object level provided information related to the intrinsic properties of an object. Alternatively at the context level, each object is characterized according to the properties of the *surrounding/neighbouring* objects. The attributes derived at the context level have been alternatively referred in the literature as external context attributes (Hermosilla et al., 2012) or geographic object-based image-texture (GEOTEX) (Chen et al., 2011; Powers et al., 2012).

Because many descriptive attributes were computed, it was first necessary to reduce this number before the creation of the classification rules. The refinement of the attributes was carried out using the winnow algorithm (Littlestone, 1988). This process numerically estimates the importance of the descriptive attributes for the particular problem analyzed, thereby enabling the identification of only the most useful attributes. These selected attributes were then ranked in order of significance based on the degree by which misclassification cost would increase if that attribute were excluded.

The objects were classified using the C5.0 algorithm, an advanced version (Kuhn and Johnson, 2013) of the C4.5 algorithm (Quinlan, 1993). In simple terms, this algorithm classifies each object as one of the five classes (*bog*, *fen*, *forest*, *shrub*, or *industrial disturbance*) by using the reference data (i.e. training samples) to construct decision trees. A decision-tree is a set of conditions organized in a hierarchical structure (Breiman et al., 1984). How the objects meet these conditions, based on their attributes, will determine which class it is assigned. During the classification, a pruning

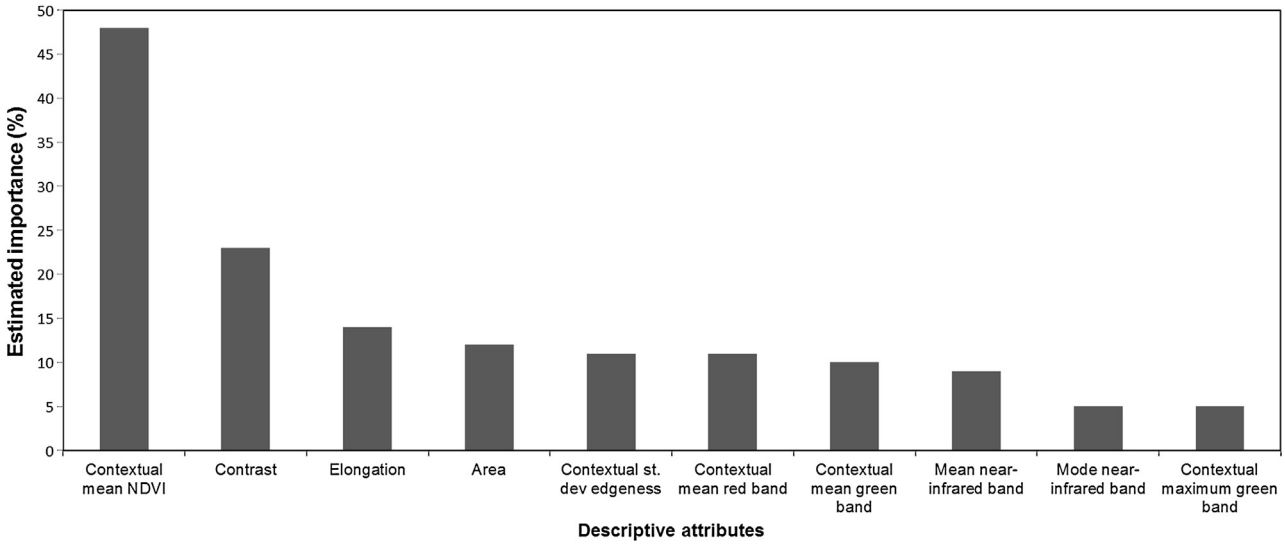

Fig. 3. Ten first attributes selected by the winnowing algorithm ranked by their classification estimated importance.

process was used to improve the predictive accuracy by reducing over-fitting. Pruning constrains how the initial tree fits the training data by fixing the minimum number of training cases each node (leaf) must contain before splitting (branching) into two subsets – here a minimum of three cases were required per node. Following the pruning, those parts of the decision trees (sub-tree, leaf or sub-branch) with a relatively high error rate were removed. After this stage, the overall performance of the tree as a whole was assessed (Murthy, 1998).

Decision trees were applied in combination with the boosting technique, which increases classifier accuracy by constructing 10 decision trees (Freund and Schapire, 1995). This technique is based on the assignment of weights to the training samples, whereby samples with greater weight have more influence on the classifier. After each tree construction, the weights are adjusted to reflect the model performance. Specifically, erroneously classified samples maintain their assigned weights, whereas the weights of correctly classified samples are reduced. Thus, the model obtained in the next iteration is more relevant than the previous. After constructing the decision-tree set, the objects were assigned a "final" class based on the combined weights and estimated error.

We assessed the accuracy of the classification model using a leave-one-out cross-validation which selects one object as validation data from the sample set and then uses the remaining data to train the classification. This process iterates until every object is selected as validation data (Fukunaga, 1990). The overall, user's and producer's accuracy were derived using a confusion matrix (Congalton, 1991).

Results and discussion

The classification achieved a high overall accuracy of 88%, with user's accuracies ranging from 84 to 92% and producer's accuracies 77 to 94% (Table 1). The greatest inter-class confusion occurred between *industrial disturbance* and *shrub*, as the partial recovery of some disturbances obscured its geometry and produced a similar vegetation composition with a comparable spectral response as *shrub*. To a lesser extent, *industrial disturbances* were also confused with the *fen* class. Within the study area there was a variety of fen types (e.g., treed rich, shrubby poor, shrubby rich, etc.) some of which contained a large arbustive component; consequently, some confusion between *fen* and *shrub* occurred. In the same sense, while both *bog* and *fen* wetland classes differ with respect to moisture, nutrient and hydrodynamic regimes, they can comprise of similar vegetation compositions (e.g., shrubby bog and shrubby poor fen) which lead to some minor confusion. The *forest* class is the most structurally and spectrally distinct, and subsequently also had the highest accuracy.

The outcomes of the winnow algorithm application are shown in Fig. 3, which shows the 10 most relevant descriptive attributes from all the defined groups (i.e., spectral, texture and geometrical properties) at both the object and context levels. The most effective descriptive attribute was the contextual mean NDVI, which provides information about the condition and productivity of adjacent vegetation. Other relevant contextual descriptive attributes included the edgeness standard deviation, the mean red channel, and the minimum and maximum green channel. The fact that half of the most relevant descriptive attributes were contextual in nature implied that the additional spatial information aided class separation by providing a framework for contextualizing the differences of the classes. The elongation and area geometrical attributes were also found to be highly relevant descriptors. What makes geometrical attributes unique among the other ranked groups (i.e., spectral and texture), is that they are characterized by the object itself, not the context. When classifying uniquely shaped objects (e.g., industrial disturbances like roads, structures, well sites and seismic lines), it is logical that accounting for geometrical properties, such as shape and dimension, can improve the discrimination of these features better than information gleaned by neighbouring objects. The second most relevant descriptive attribute was the object-level contrast texture, which informs on the amount of variation between low and high values that exists within an object. Specifically, this texture quantified the structure and spatial distribution of vegetation and other scene elements, which was particularly useful for differentiating objects that are functionally different, but spectrally similar.

Fig. 4 provides three examples that illustrate the technique's performance under different landscape conditions. Fig. 4(a) shows clearly defined industrial disturbances juxtaposed over forest and shrub land cover types. In forested regions the industrial disturbances were clearly captured by both the segmentation and classification. There was some confusion observed in identifying industrial disturbances in shrub dominated areas, because some natural disturbances were also misclassified as industrial disturbances (Fig. 4, a1). Since some fine-scale natural disturbance features (e.g., riverbank erosion and minor landslides) may share

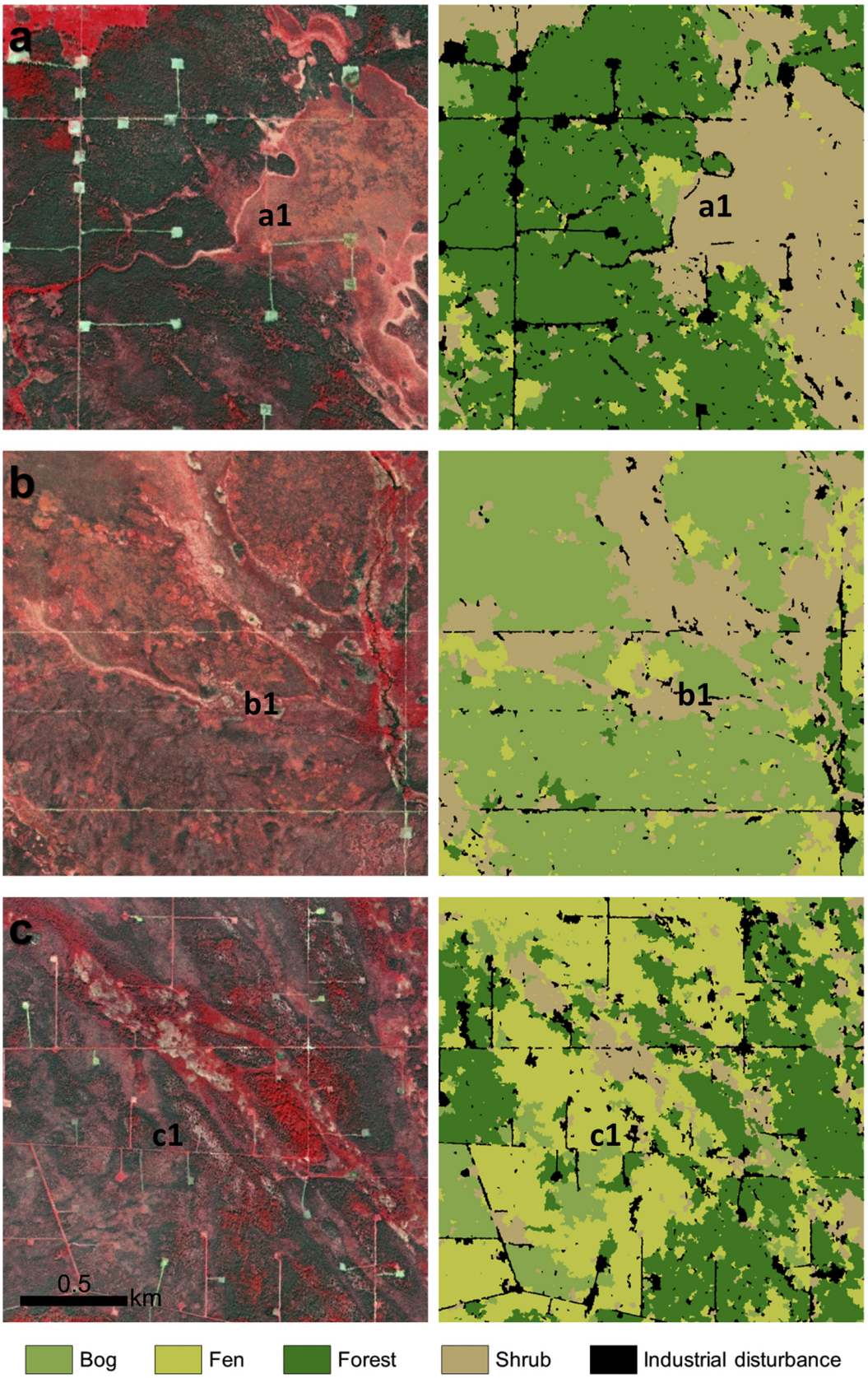

Fig. 4. SPOT5 imagery (left) and corresponding classification (right) for locations with (a) clearly defined industrial disturbances in a forest and shrub dominated landscape; (b) industrial disturbances in a bog and shrub dominated landscape; and (c) a fragmented landscape and many instances of industrial disturbances at various stages of recovery. The locations a1, b1, and c1 represent areas where there was confusion observed in identifying industrial disturbances.

Table 1
Confusion matrix of the classification.

	Reference						
	Bog	Fen	Forest	Shrub	Industrial disturbance	Total	User's accuracy
Bog	70	2	3	1	2	78	89.7
Fen	9	231	4	17	12	273	84.6
Forest	5	5	170	2	5	187	91
Shrub	3	13	2	171	15	204	83.8
Industrial disturbance	3	9	1	27	453	493	92
Total	90	260	180	218	487	1235	
Producer's accuracy	77.8	88.9	94	78.4	93		
Overall accuracy 88.7%							

many of the same traits (e.g., spectral and geometrical) as industrial, we foresee challenges in separating these disturbances. However, it should be noted that industrial disturbance features are, in many cases, quite distinct with respect to their shape and spatial continuity. As such, while their unique shape (e.g., angular, narrow or linear) and continuity remain, industrial features are distinguishable from other classes, even those with similar land cover appearance.

Fig. 4(b) provides an example of industrial disturbances within a bog and shrub dominated landscape. Defining industrial disturbances in their entirety was made challenging due to advanced stages of recovery, more so in the presence of shrubs (Fig. 4, b1). However, industrial disturbance features, like the well site and two of the seismic lines, retained their shape and continuity characteristics and were identified. The GEOBIA approach presented could be used with high spatial resolution time series datasets to analyze vegetation recovery over time, which in turn could improve the detection of subtle disturbances. Fig. 4(c) shows a fragmented landscape impacted by many industrial disturbances at various stages of recovery. It is evident that some industrial disturbances were not properly captured (Fig. 4, c1). Specifically, challenges associated with segmentation and the process of applying a discrete boundary on a continuous landscape produced ambiguous boundaries for some industrial disturbances. For example, the separation between disturbed and undisturbed areas can be less apparent in older industrial disturbances. This ambiguity surrounding the identification of object boundaries can lead to inaccurate segmentation, as has already been reported by Montaghi et al. (2013). However, a benefit of the segmentation method performance is that it ignores the size homogeneity of the objects produced, which entails the definition of objects with significantly dissimilar sizes. This feature enabled the creation of small-sized polygons that were able to enclose industrial disturbances without resulting in over-segmentation of larger natural covers typically produced by other algorithms (Schiewe, 2002; Corcoran and Winstanley, 2008). This capability is particularly useful for this and similar research, that attempts to classify fine-scale features amongst vast areas of continuous natural landscapes (e.g., expansive wetlands, forests and shrub dominated landscapes).

Future work might explore other classification techniques (e.g., random forest, support vector machines, neuronal networks) and/or additional indicators that may enable better separation specifically between industrial disturbances and those fine-scale natural disturbances that exhibit similar shape and spectral properties. Additionally, it might be beneficial to explore other accuracy assessment approaches, besides the traditional thematic error matrix, that are specific to classifications based on objects. These approaches (e.g., object fate analysis (OFA) by Schöpfer et al. (2008), and Purity Index by Van Coillie et al. (2008)) could be used to more fully assess the accuracy of the object-based maps and potentially improve classification. For example, the OFA-matrix approach presented by Hernando et al. (2012) can assess both the thematic and spatial accuracies simultaneously; thus, is able to capture thematic and spatial relationships.

Conclusions

In this paper we presented and assessed a GEOBIA approach for mapping fine-scale industrial disturbances. Identifying the location of these disturbances can provide important information for decision makers, planners, and resource managers who need to monitor the state of forest condition, composition and extent within multi-use landscapes. Using a watershed by immersion segmentation algorithm, we were able to create image objects, which were then characterized with spectral, texture and geometrical attributes, in addition to their contextual properties. A winnow algorithm was next applied to determine which descriptive attributes were the most relevant for the classification. Finally, the objects were classified using decision trees constructed with the C5.0 algorithm together with the boosting technique. We found that the proposed GEOBIA approach produced accurate classification results with an overall accuracy of 88%. Furthermore, the outcomes highlight the complementary nature of the descriptive attribute set, where descriptors of all three defined groups (i.e., spectral, texture and geometrical properties) at both the object and context levels were shown to be highly relevant for the classification. While our results indicate that there were some challenges distinguishing between industrial disturbances (e.g., at advanced stages of recovery) and fen wetlands, our approach did enable the identification and classification of fine-scale industrial disturbances. The approach presented could also be used to investigate the impacts of these disturbance types on landscape pattern and wildlife, which in turn could be useful for aiding effective environmental management and conservation in affected areas.

Acknowledgements

This article was jointly funded by the Natural Sciences and Engineering Research Council of Canada, the University of British Columbia and the mobility grant provided by the Erasmus Mundus Programme of the European Commission under the Transatlantic Partnership for Excellence in Engineering – TEE Project.

References

Archibald, W.R., Ellis, R., Hamilton, A.N., 1987. Responses of grizzly bears to logging truck traffic in the Kimsquit River Valley, British Columbia. Bears: Biol. Manage. 7, 251–257.

Balaguer-Beser, A., Ruiz, L.A., Hermosilla, T., Recio, J.A., 2013. Using semivariogram indices to analyse heterogeneity in spatial patterns in remotely sensed images. Comput. Geosci. 50, 115–127.

Blaschke, T., Hay, G.J., Kelly, M., Lang, S., Hofmann, P., Addink, E., Feitosa, R., Van Der Meer, F., Van Der Werff, H., Van Coillie, F., Tiede, D., 2014. Geographic object-based image analysis: a new paradigm in remote sensing and geographic information science. ISPRS Int. J. Photogrammet. Remote Sens. 87, 180–191.

Blaschke, T., Strobl, J., 2001. What's wrong with pixels? Some recent developments interfacing remote sensing and GIS. GeoBIT/GIS 6, 12–17.
Benz, U.C., Hofmann, P., Willhauck, G., Lingenfelder, I., Heynen, M., 2004. Multi-resolution, object-oriented fuzzy analysis of remote sensing data for GIS-ready information. ISPRS J. Photogrammet. Remote Sens. 58, 239–258.
Breiman, L., Friedman, J., Stone, C.J., Olshen, R.A., 1984. Classification and Regression Trees. CRC Press.
Chartfield, C., 1991. Avoiding statistical pitfalls. Stat. Sci. 6, 240–252.
Chen, G., Hay, G.J., Castilla, G., St-Onge, B., Powers, R., 2011. A multiscale geographic object-based image analysis to estimate lidar-measured forest canopy height using Quickbird imagery. Int. J. Geogr. Inform. Sci. 25, 877–893.
Congalton, R.G., 1991. A review of assessing the accuracy of classifications of remotely sensed data. Remote Sens. Environ. 37, 35–46.
Corcoran, P., Winstanley, A., 2008. Using texture to tackle the problem of scale in land-cover classification. In: Object-based Image Analysis. Springer, Berlin, pp. 113–132.
Desclée, B., Bogaert, P., Defourny, P., 2006. Forest change detection by statistical object-based method. Remote Sens. Environ. 102, 1–11.
Freund, Y., Schapire, R.E., 1995. A decision-theoretic generalization of on-line learning and an application to boosting. In: Computational Learning Theory. Springer, Berlin, pp. 23–37.
Fukunaga, K., 1990. Statistical Pattern Recognition. Academic Press, New York.
Gillanders, S.N., Coops, N.C., Wulder, M.A., Gergel, S.E., Nelson, T., 2008. Multitemporal remote sensing of landscape dynamics and pattern change: describing natural and anthropogenic trends. Prog. Phys. Geogr. 32, 503–528.
Government of Alberta (GOA), 1998. Exploration Regulation, AR 214/98, sec. 43, http://www.canlii.org/ (accessed 01.04.14).
Haralick, R.M., Shanmugam, K., Dinstein, I.H., 1973. Textural features for image classification. IEEE Trans. Syst. Man Cybernet. 6, 610–621.
Hay, G.J., Castilla, G., 2008. Object-based image analysis—spatial concepts for knowledge-driven remote sensing applications. In: Blaschke, T., Lang, S., Hay, G.J. (Eds.), Geographic Object-Based Image Analysis (GEOBIA). Springer-Verlag, Berlin, pp. 77–92.
Hay, G.J., Castilla, G., Wulder, M.A., Ruiz, J.R., 2005. An automated object-based approach for the multiscale image segmentation of forest scenes. Int. J. Appl. Earth Observ. Geoinform. 7, 339–359.
Hernando, A., Tiede, D., Albrecht, F., Lang, S., 2012. Spatial and thematic assessment of object-based forest stand delineation using an OFA-matrix. Int. J. Appl. Earth Observ. Geoinform. 19, 214–225.
Hermosilla, T., Ruiz, L.A., Recio, J.A., Cambra-López, M., 2012. Assessing contextual descriptive features for plot-based classification of urban areas. Landsc. Urban Plann. 106, 124–137.
Hobson, K.A., Bayne, E., 2000. Effects of forest fragmentation by agriculture on avian communities in the southern boreal mixedwoods of western Canada. Wilson Bull. 112, 373–387.
Johansen, K., Arroyo, L.A., Phinn, S., Witte, C., 2010. Comparison of geo-object based and pixel-based change detection of riparian environments using high spatial resolution multi-spectral imagery. Photogrammet. Eng. Remote Sens. 76, 123–136.
Kuhn, M., Johnson, K., 2013. Applied Predictive Modeling. Springer, New York.
Laben, C.A., Bernard, V., Brower, W., 2000. Process for Enhancing the Spatial Resolution of Multispectral Imagery Using Pan-sharpening. U.S. Patent No. 6,011,875. U.S. Patent and Trademark Office, Washington, DC.
Linke, J., Franklin, S.E., Huettmann, F., Stenhouse, G.B., 2005. Seismic cutlines, changing landscape metrics and grizzly bear landscape use in Alberta. Landsc. Ecol. 20, 811–826.
Littlestone, N., 1988. Learning quickly when irrelevant attributes abound: a new linear-threshold algorithm. Mach. Learn. 2, 285–318.
Mace, R.D., Waller, J.S., Manley, T.L., Lyon, L.J., Zuuring, H., 1996. Relationships among grizzly bears, roads and habitat in the Swan Mountains, Montana. J. Appl. Ecol. 33, 1395–1404.
Meddens, A.J., Hudak, A.T., Evans, J.S., Gould, W.A., González, G., 2008. Characterizing forest fragments in boreal, temperate, and tropical ecosystems. AMBIO: J. Hum. Environ. 37, 569–576.
Montaghi, A., Larsen, R., Greve, M.H., 2013. Accuracy assessment measures for image segmentation goodness of the Land Parcel Identification System (LPIS) in Denmark. Remote Sens. Lett. 4, 946–955.
Murthy, S.K., 1998. Automatic construction of decision trees from data: a multi-disciplinary survey. Data Min. Knowl. Discov. 2, 345–389.
Osko, T., MacFarlane, A., 2001. Natural Reforestation on Seismic Lines and Well Sites in Comparison to Natural Burns or Logged Sites. Alberta-Pacific Forest Industries, Boyle, Alberta.
Potapov, P., Turubanova, S., Hansen, M.C., 2011. Regional-scale boreal forest cover and change mapping using Landsat data composites for European Russia. Remote Sens. Environ. 115, 548–561.
Powers, R.P., Hay, G.J., Chen, G., 2012. How wetland type and area differ through scale: a GEOBIA case study in Alberta's Boreal Plains. Remote Sens. Environ. 117, 135–145.
Quinlan, J.R., 1993. C4.5. Programs for machine learning. Morgan Kaufmann, San Mateo.
Robinson, D.J., Redding, N.J., Crisp, D.J., 2002. Implementation of a Fast Algorithm for Segmenting SAR Imagery. Scientific and Technical Report No. DSTO-TR-1242. Electronics Research Lab, Australia, Salisbury.
Ruiz, L.A., Recio, J.A., Fernández-Sarría, A., Hermosilla, T., 2011. A feature extraction software tool for agricultural object-based image analysis. Comput. Electron. Agric. 76, 284–296.
Schneider, R.R., 2002. Alternative Futures. Alberta's Boreal Forest at the Crossroads. The Federation of Alberta Naturalists and the Alberta Centre for Boreal Research, Edmonton.
Schneider, R., Dyer, S., 2009. Death by a Thousand Cuts: The Impacts of in situ Oil Sands Development on Alberta's Boreal Forest. The Pembina Institute for Appropriate Development.
Schiewe, J., 2002. Segmentation of high-resolution remotely sensed data-concepts, applications and problems. Int. Arch. Photogrammet. Remote Sens. Spatial Inform. Sci. 34, 380–385.
Schöpfer, E., Lang, S., Albrecht, F., 2008. Object-fate analysis: spatial relationships for the assessment of object transition and correspondence. In: Blaschke, T., Lang, S., Hay, G.J. (Eds.), Geographic Object-Based Image Analysis (GEOBIA). Springer-Verlag, Berlin, pp. 786–801.
Schroeder, T.A., Wulder, M.A., Healey, S.P., Moisen, G.G., 2011. Mapping wildfire and clearcut harvest disturbances in boreal forests with Landsat time series data. Remote Sens. Environ. 115, 1421–1433.
Sobel, I., Feldman, G., 1968. A 3×3 isotropic gradient operator for image processing. Talk at the Stanford Artificial Project: 271-272.
Severson-Baker, C., 2004. Environment and Energy in the North Primer Series. The Pembina Institute for Appropriate Development.
Van Coillie, F.M.B., Verbeke, L.P.C., De Wulf, R.R., 2008. Object-based image analysis for remote sensing applications: modeling reality-dealing with complexity. In: Blaschke, T., Lang, S., Hay, G.J. (Eds.), Geographic Object-Based Image Analysis (GEOBIA). Springer-Verlag, Berlin, pp. 237–256.
Vincent, L., Soille, P., 1991. Watersheds in digital spaces: an efficient algorithm based on immersion simulations. IEEE Trans. Pattern Anal. Mach. Intell. 13, 583–598.
Wulder, M.A., White, J.C., Hay, G.J., Castilla, G., 2008. Towards automated segmentation of forest inventory polygons on high spatial resolution satellite imagery. For. Chron. 84, 221–230.
Wulder, M.A., Hall, R.J., Coops, N.C., Franklin, S.E., 2004. High spatial resolution remotely sensed data for ecosystem characterization. BioScience 54, 511–521.
Zager, P., Jonkel, C., Habeck, J., 1983. Logging and wildfire influence on Grizzly Bear habitat in northwestern Montana. Bears: Biol. Manage. 5, 124–132.
Zhou, W., Troy, A., 2008. An object-oriented approach for analysing and characterizing urban landscape at the parcel level. Int. J. Remote Sens. 29, 3119–3135.